ORIGINAL SCIENTIFIC PAPER

CROATICA CHEMICA ACTA

Croat. Chem. Acta **2019**, *92*(1), 59–68
Published online: February 26, 2019
DOI: 10.5562/cca3463

HKD 1926

Hydroxyapatite/Silver Nanoparticles Powders as Antimicrobial Agent for Bone Replacements

Agnieszka Sobczak-Kupiec, Dagmara Malina, Regina Kijkowska, Wioletta Florkiewicz,* Klaudia Pluta, Zbigniew Wzorek

Institute of Inorganic Chemistry and Technology, Cracow University of Technology, 31-155 Cracow, Poland

* Corresponding author's e-mail address: florkiewicz@chemia.pk.edu.pl

RECEIVED: December 5, 2018 ✶ REVISED: February 18, 2019 ✶ ACCEPTED: February 18, 2019

Abstract: This paper reports a superficial morphological modification of the hydroxyapatite grains obtained by *in situ* deposition of Ag nanoparticles on natural origin calcium phosphate powder. Ceramic material was prepared in three stage bone treatment, including hydrolysis with a lactic acid, pre-calcination, and proper calcination. Subsequently, the Ag nanoparticles were synthesized by chemical reduction of Ag^+ by sodium borohydride in a solution of polyvinylpyrrolidone and in presence of hydroxyapatite. Such-prepared materials were investigated with X-ray diffraction, Fourier-transformed infrared spectroscopy, atomic absorption spectrometry and scanning electron microscopy with energy dispersive spectroscopy. Furthermore, Ca/P molar ratio was calculated and microbiological tests were performed to investigate materials antimicrobial activity. The appearance of Ag nanoparticles located on phosphate surface was confirmed by SEM analysis, and no chemical bonding with hydroxyapatite was recorded by IR and XRD techniques. Additionally, the biological assessment revealed bactericidal effect on *Escherichia coli* and *Staphylococcus aureus*, while slightly affected on *Enterococcus faecalis* viability.

Keywords: hydroxyapatite, silver nanoparticles, antibacterial activity, surface modification.

INTRODUCTION

As the civilizational development progresses, the number of people aged 65 and above increases making the population aging a global issue.[1–2] The number of retirement-age people is predicted to double by 2050, thus the increasing demand for implant materials resulting from population aging and unceasing health-care improvement as well is understandable. The main requirements of biomedical materials relating to their biological properties and strength, among which the most important are biomechanical compatibility, biofunctionality, bioactivity, and for materials implanted for a limited time, also bioresorption.[3–4] However, interference with the patient's body often leads to postoperative infections, which entails re-surgery. Specially design biomaterials combining features which help maintain the properties and architecture of the natural tissue, possessing antimicrobial properties providing sterility during the adaptation of an implant and enhancing healing of the postoperative wound, can be the reasonable solution for the re-surgeries problem.

The highest biocompatibility and ability to support cell growth among all implant materials were found in the hydroxyapatite bioceramic which is generally recognized as a non-toxic and biologically active material.[5–7] Nevertheless, bioceramics have no antimicrobial properties, thus re-surgery caused by infections related to the opening of tissues during the implantation procedure is often needed despite the full biocompatibility of material. This may be resolved by the use of ions and metal particles providing biocidal properties. If they were used for implantation purposes together with the biocompatible bioceramics, a locally antimicrobial and bioactive material could be introduced into the organism. Silver is an element with strong biocidal properties associated with the process of gradual oxidation of silver atoms on the sample surface in the presence of oxygen and atmospheric water. Silver ion on animal biologically active surfaces is deactivated through the reduction to insoluble forms, while nanosized silver does not react with salts in biological liquids, which accounts for its extraordinary disinfecting efficacy. The biocidal activity of silver nanoparticles depends on their size and shape. The spatial network of silver crystal

contains atoms that can react with the environment. Still, as the size of the silver crystalline network increases, the number of inactive atoms grows as well because part of the atoms is locked inside the crystallite and thus unable to react with the environment.[8–10] It has been demonstrated that silver, apart from its antibacterial properties, in the hydroxyapatite/Ag powders significantly improves a number of unfavorable mechanical properties. Hydroxyapatite modified with metallic silver sintered in an air atmosphere has a higher modulus of elasticity and lower hardness than hydroxyapatite itself. Studies performed by M. Diaz confirmed the antibacterial activity of the HA/Ag^+ powders towards *Staphylococcus aureus*, *Pneumococcus*, and *Escherichia coli*.[11] X. Zhang et al. described in their studies HA/Ag^+ materials prepared using mechanochemical methods from a mixture of hydroxyapatite and silver oxide powders sintered at 1250 °C.[12] Hydroxyapatite containing metallic silver can be obtained through the chemical reduction using polyvinyl alcohol as the stabilizer and dimethylformamide as the reducing agent as well.[13] Silver-modified hydroxyapatite can also be obtained using the sol-gel method with silver oxide and citric acid in the presence of ammonia solution.[14] Studies carried out by Rameshbabu et al.[15] and Fakharzadeh et al.[16] demonstrated the increased efficacy of implanTable biomaterials used to manage bone damage that contains silver. The literature contains numerous examples of ways to obtain silver compound-modified bioceramics but there are no records describing calcium phosphates modified with silver nanoparticles. It is worth noting that even high biocompatibility and proper fitting of the implant to the bone defect, do not overcome the fact that every intervention in the living organism causes a number of changes in the patient's body. Furthermore, one of the obstacles of all types of surgery is postoperative complications consisting mainly of inflammation at the surgical site. In order to minimize the probability of such a phenomenon, the authors plan to developed materials antibacterial and antifungal properties by introducing nanosized silver with increased antimicrobial properties as compared to silver ions. In general, these nanoparticles do not affect mammalian cells containing peptidoglycans. However, it is proved, that metallic nanoparticles destroy the bacteria cells in a few stages including penetration of its interior, surrounding the bacteria with tight layer, blocking flagella, fimbriae, and pils, leading to the inability of bacteria to move, and eliminating contact with other bacteria cells resulting in no genetic material exchanging and finally losing the ability to reproduction. Based on previous original studies by the authors,[17] this paper attempts to obtain hydroxyapatite crystals coated with silver nanoparticles. Metallic nanoparticles were obtained in a chemical reduction in the presence of hydroxyapatite (*in situ* method). The procedure resulted in carbonated hydroxyapatite (cHA) powders with silver nanoparticles without significant morphological changes to the original material. The presented study on the synthesis and application of this type of biomaterial may prove to become an important step towards a new generation of bioactive materials intended to medical and dental application that are burdened with only a small probability of postoperative complications; low costs, simple process conditions, and no need for complicated equipment are unquestionable advantages of the proposed technology.

MATERIALS AND METHODS

Natural hydroxyapatite was prepared in a three-stage process involving hydrolysis with the lactic acid, precalcination (650 °C), and proper calcination (900 °C) in chamber furnace in an air atmosphere as described by Sobczak-Kupiec et al.[18] The cHA surface was modified by obtaining silver nanoparticles (AgNPs) *in situ*. To this end, 6 g of natural origin hydroxyapatite (sieve fraction below 65 μm) was introduced into 40 mL of 3 % water solution of polyvinylpyrrolidone (PVP, M.W. 8000, Alfa Aesar, reagent grade) while stirring. Next, silver(I) nitrate (POCH, reagent grade) was introduced into the suspension in the amount equivalent to Ag concentrations of 500 ppm (0.0394 g) (cHA500) and 1000 ppm (0.0788 g) (cHA1000). A reducing agent, sodium borohydride (POCH, reagent grade) at a molar ratio of 1:10 to silver ions (0.1490 g or 0.0279 g) was dissolved in 10 mL of the PVP solution (3 %) and added dropwise into the prepared mixture. The modification was introduced at room temperature with stirring continued for 15 minutes after the completion of the introduction of the reducing agent. Immediately after the $NaBH_4$ solution was dosed, the suspension changed its color from white to brown-grey. The suspension was eventually filtered, flushed with deionized water, and dried at room temperature.

The resulting materials were subjected to X-ray diffraction XRD analysis to determine the phase composition of the materials, scanning electron microscopy with X-ray microanalysis EDS, spectrum analysis using the FT-IR method, determination of silver content using atomic absorption spectroscopy (AAS) with Analyst 300 by PerkinElmer, and determination of Ca and P in accordance with Polish standards PN-R-64803:199P and PN-80/C-87015.[19,20] Qualitative phase analysis of prepared materials was performed using powder X-ray Diffractometry utilizing XRD - Philips X'Pert diffractometer with Cu Kα radiation (λ = 0.15418 nm), equipped with graphite monochromator PW 1752/00 operating at 40 kV and 30 mA. Scans were performed over Bragg-Brentano geometry in the 2θ range of 10 ° to 60 ° with scanning speed 0.05 °/s

using standard holder (20×10×2 mm). The Match! software version 3.6 with reference patterns calculated from the COD database was performed for phase identification from powder diffraction data. In order to fully characterize the chemical composition of cHA and cHA/AgNPs materials, Fourier-transform infrared spectroscopy was utilized. Materials were investigated with Scimitar Series Digilab FT-IR Spectrometer in the range of middle infrared of 400-4000 cm^{-1}. Morphology and chemical composition of cHA samples placed on the copper holder and sputter–coated with gold were investigated with scanning electron microscope (SEM) with energy dispersive detector under vacuum. SEM images were obtained using a JEOLJSM-5510L with energy dispersive spectroscopy (EDS) at the accelerating voltage of 15 kV. Calcium content in all powders was assayed using complexometric titration with ethylenediaminetetraacetic acid (EDTA). The method employed the mineralization of the sample in nitric acid, precipitating phosphates with bismuth(III) nitrate, and then determining calcium by EDTA titration in the presence of indicator (calcein and thymolphthalein). Phosphorus content in the material was determined using the spectrophotometric method. This method involves the production of a phosphorus-vanadium-molybdenum complex and the photometric measurement of the optical density at the wavelength of 430 nm. The analysis was performed on spectrophotometer Evolution 201 by ThermoScientific.

To fully address the question, whether obtained surface-modified carbonated hydroxyapatite have antibacterial activity, we performed antimicrobial studies against three respective pathogenic organisms, *Staphylococcus aureus* (ATCC 25923), *Escherichia coli* (ATC 25922) and *Enterococcus faecalis* (ATCC 29212). *S. aureus* is an abundant Gram(+) bacteria, typically found in nasal passages and ears of patients.[21] This bacteria is recognized to be a significant factor initializing localized and systemic infections including osteomyelitis[22] and chronic wound infection,[23] as well as dental implant infections.[24] Infections caused by Gram(–) bacteria account for ~15 % of Orthopaedic Implant Infections (OII) which is related with the increase in treatment failure risk and *E. coli* is the second most common Gram(–) bacteria causing OII.[25] The Gram(+) bacteria *E. faecalis* are usually found in the gastrointestinal tract of humans. Nonetheless, colonization of the genitourinary tract and the oral cavity are also reported. *E. faecalis* is the most common bacteria found in infected root canals and marginal periodontitis.[26] Prior to the experiments, microbial suspensions were adjusted to a density of 1×10^5 CFU/mL obtained from 18 h bacterial cultures developed on solid media. The antimicrobial studies against *E. coli* and *S. aureus* were tested on Muller Hinton Agar medium, while Muller Hinton Agar containing 5 % of sheep blood was used in case of *E. faecalis*. The tested powders were suspended in DMSO at the concentration of 100 mg/mL. 100 µL of prepared material was then placed in triplicate in test tubes containing 100 µL of bacterial suspension and 800 µL 0.9 % NaCl and incubated in 37 °C for 24 hours. The test tubes containing 100 µL of NaCl solution instead of the tested substances were used as a growth control. After the incubation, the number of colonies grown was counted and compared to the control (C) that represented 100 % growth. The tests were carried out based on the procedures included in the Polish standards PN-EN 1040:2006E and PN-EN 1276:2010E.[27,28] Additionally, the agar diffusion assay was used to test the sensitivity of bacteria to the prepared hydroxyapatite powders modified with silver nanoparticles. In this method discs to test the extent to which bacteria strains are affected by tested materials. If the bacterial strain is susceptible to the tested substances, then a wide ring of no bacterial growth appears on the agar plate, while an ineffective antimicrobial substance will show no change in the surrounding media at all. With this method, microbial suspensions corresponding to a 0.5 McFarland density was seeded into sterile Petri plates containing Mueller Hinton agar medium. Then, 10 µL of 100 mg/mL hydroxyapatite-AgNPs suspensions were loaded on 9 mm diameter sterile disks (in triplicate), which next where placed on the Petri dish and incubated for 24 h at 37 °C. The results were recorded by observing the inhibition zone.

The significant differences between control and treated cells were statistically analyzed by independent-sample Student's t-test. The analysis was conducted in Statistica 13.1 PL software (StatSoft, Poland). Results were considered statistically significant when $p < 0.05$.

RESULTS

X-ray Diffraction Analysis

In order to determine phase composition of the analyzed materials X-ray diffractometry was used. X-ray diffraction patterns of pure cHA and cHA/NPs powders are shown in Figure 1.

The diffraction patterns suggest that the cHA was highly crystalline, which was indicated by the presence of sharp peaks. The analysis has demonstrated that the only crystalline phase in the material is hydroxyapatite.

FT-IR Analysis

In order to fully characterize chemical composition of cHA and cHA/AgNPs materials Fourier-transform infrared spectroscopy was utilized. IR spectra of cHA and cHA/AgNPs powders are shown in Figure 2 and summarized in Table 1.

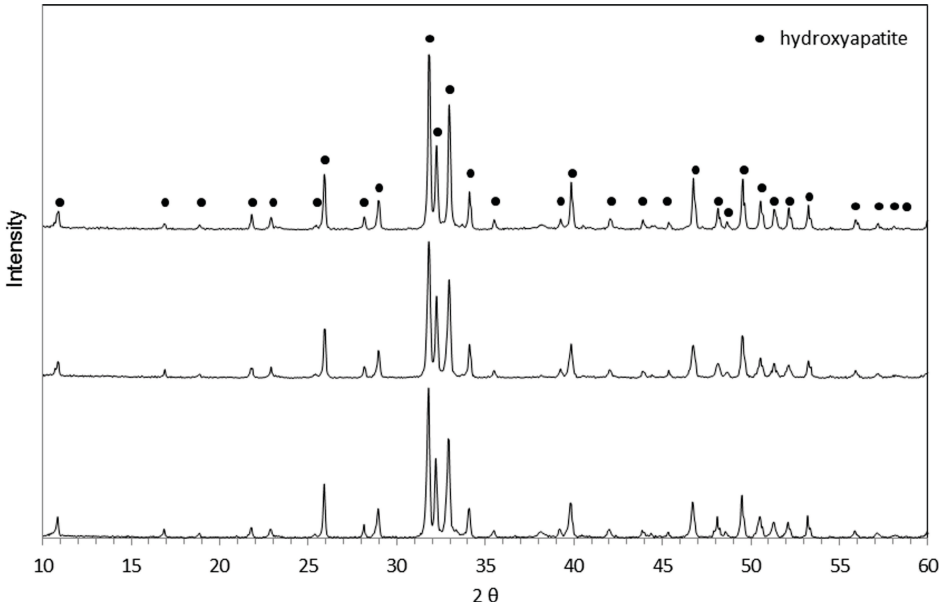

Figure 1. X-ray diffraction patterns of cHA, cHA500 and cHA1000 powders.

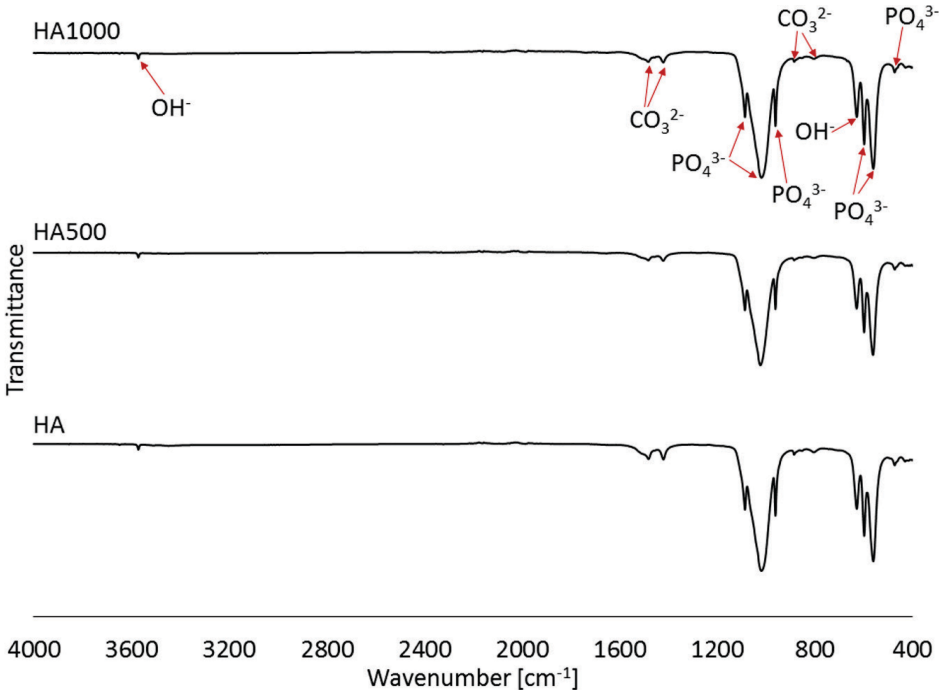

Figure 2. IR spectra of natural cHA and cHA/AgNPs powders.

In the 1000–1100 cm^{-1} region, bands located at 1037 cm^{-1} and 1090 cm^{-1} were attributed to the v_3 triply degenerate asymmetric stretching mode of PO_4^{3-}. The transmittance band at 963 cm^{-1} was assigned to the v_4 bending vibration of phosphate (PO_4^{3-}). Furthermore, two distinctive peaks observed at 627 cm^{-1} and 3568 cm^{-1} were attributed to in-plane vibration δ of OH^- and v_s stretching mode of the structural OH^- anion, respectively. Two sharp and intensive bands in the low wavenumber region at 601 cm^{-1} and 568 cm^{-1} correspond to v_4 triply degenerate bending mode of PO_4^{3-}, while the band at 470 cm^{-1} represents v_2 doubly degenerate bending mode of PO_4^{3-}.

Table 1. IR band assignment of the samples.

Wavenumber / cm^{-1}	Peak assignment	References
3568	ν_s stretching mode of O–H	[29,30]
1489	ν_3 stretching mode of CO_3^{2-}	[29–31]
1413	ν_3 stretching mode of CO_3^{2-}	[32–34]
1090	ν_3 triply degenerate asymmetric stretching mode of PO_4^{3-} (P–O)	[19,30,32]
1032	ν_3 triply degenerate asymmetric stretching mode of PO_4^{3-} (P–O)	[30]
963	ν_1 nondegenerate symmetric stretching mode of PO_4^{3-} (P–O)	[30,34,35]
869	ν_2 bending mode of CO_3^{2-}	[30–32]
769	ν_4 in-plane deformation bending mode of CO_3^{2-} (O–C–O)	[36,37]
627	δ in-plane vibration of OH^-	[38,39]
601	ν_4 triply degenerate bending mode of PO_4^{3-} (O–P–O)	[29,32]
568	ν_4 triply degenerate bending mode of PO_4^{3-} (O–P–O)	[30,32]
470	ν_2 doubly degenerate bending mode of PO_4^{3-} (O–P–O)	[35,40]

Additionally, bands corresponding to the ν_3 stretching mode of CO_3^{2-} were detected at 1489 cm^{-1}, 1413 cm^{-1}. The weak bands at and 869 cm^{-1} and 769 cm^{-1} were also associated with presence of carbonate group in cHA structure and referring to ν_2 bending mode, and ν_4 in-plane deformation bending mode of CO_3^{2-}, respectively.

Composition Analysis

The AAS determined the amount of silver deposited on the surface of HA during the production of Ag nanoparticles with the *in situ* method. Calcium and phosphorous content in all powders was assayed using complexometric titration and spectrophotometric method, respectively. Thanks to the determination of calcium and phosphorus content in apatite, the molar ratio of Ca/P in the materials was calculated. Results are summarized in Table 2.

Molar ratios of Ca to P calculated in accordance with Polish Standards were in the range from 1.68 ± 0.11 to 1.75 ± 0.03. This demonstrates the receiving of hydroxyapatite of slightly different composition than the stoichiometric one that is characterized by Ca/P molar ratio equal to 1.67. The total silver content in the materials was 3.44 ± 0.14 mg/g for cHA500 and 5.46 ± 0.36 mg/g for cHA1000. Additionally, based on the calculated silver con-tent to the introduced value, the yield of the modification of calcium phosphate with AgNPs was calculated. As shown in Table 2, the Ca/P molar ratio in natural cHA does not change significantly after the *in situ* reduction of silver ions. The yield of the modification was 82.56 ± 4.07 % and 65.51 ± 6.59 %, for cHA500 and cHA1000, respectively.

SEM-EDS Analysis

SEM imaging gave insight into hydroxyapatite structure regarding particle size and shape. The SEM images of natural origin cHA and cHA/NPs materials taken with different magnifications are shown in Figure 3.

Figure 3A shows SEM images of natural origin HA surface. SEM imaging shows heterogeneity in cHA crystals size and shape. Spot EDS analysis indicated the presence of phosphorus, calcium, and carbon, which is typical of natural hydroxyapatite. The presence of copper and gold in EDS spectra was associated with the type of holder used in the analysis and the sputtering of powders with the conductive gold layer. SEM analysis of different points at materials surface (Figure 3D, 3G) show spherical agglomerates on apatite surface. Representative SEM images show that in both materials the synthesized AgNPs were approximating a spherical shape. In the case of sample cHA500 spherical

Table 2. Quantitative composition analysis of tested samples.

CPs material	Determined Ca/P molar ratio	Content of Ag in the sample / mg/g	Adsorbed amount of Ag / %
cHA	1.75 ± 0.03	0.00	0.00
cHA500	1.74 ± 0.08	3.44 ± 0.14	82.56 ± 4.07
cHA1000	1.68 ± 0.11	5.46 ± 0.36	65.51 ± 6.59

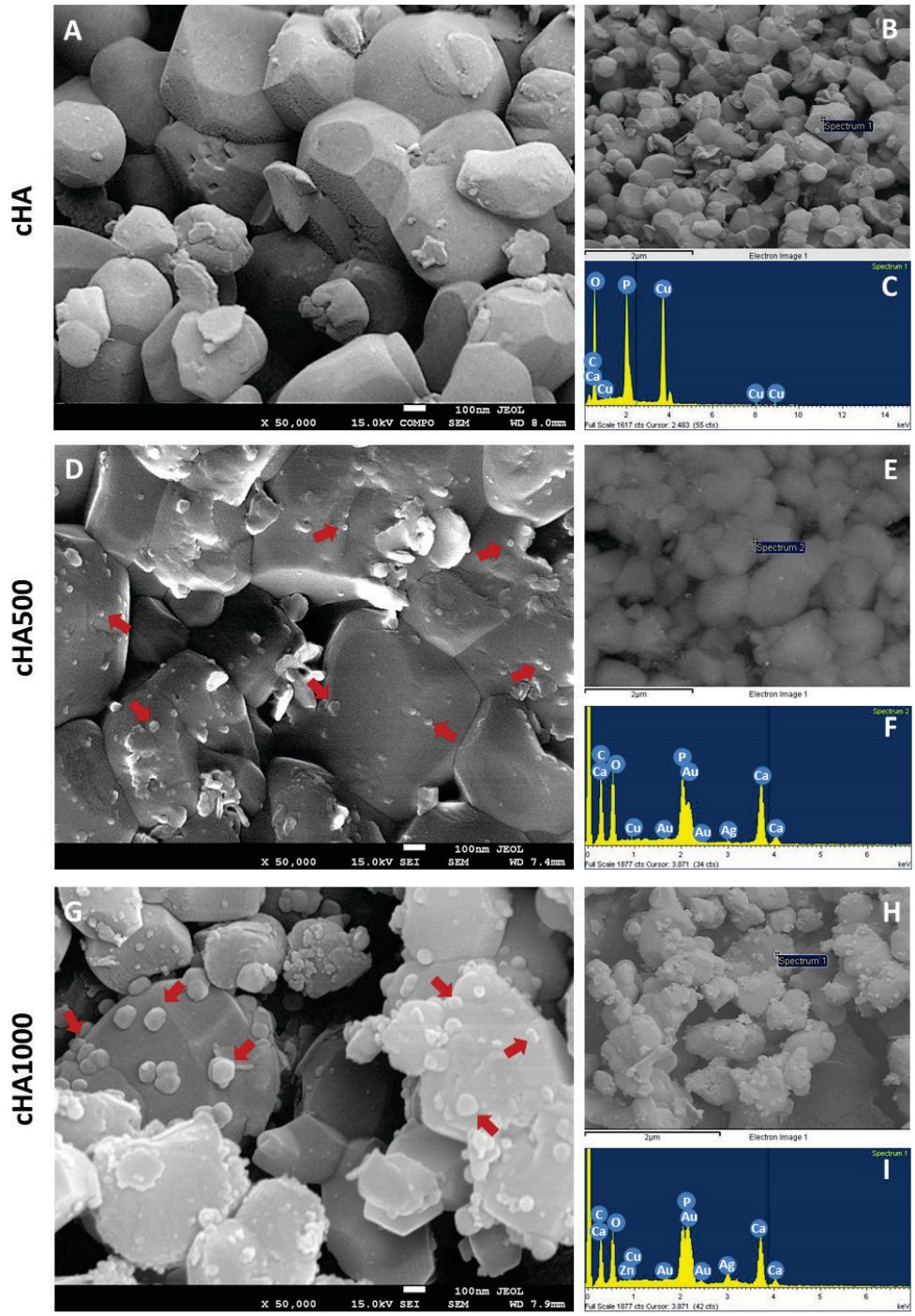

Figure 3. SEM images and EDS analysis results of cHA, cHA500 and cHA1000. Red arrows indicate AgNPs.

particles were found much smaller with a diameter of about 50 nm as shown in Figure 3D. In the case of sample cHA1000, the nanoparticles diameters were about 100 nm. What is important, the spot EDS analysis of the surfaces of modified phosphates confirmed the presence of silver in the samples.

Antibacterial Activity

Figure 4 exemplifies the bacteria growth of test species exposed to powders expressed as a percentage of viability, whose high percentage indicates poor antibacterial activity of tested materials. The symptoms of strong antibacterial reactivity were shown both in *E. coli* and *S. aureus*;

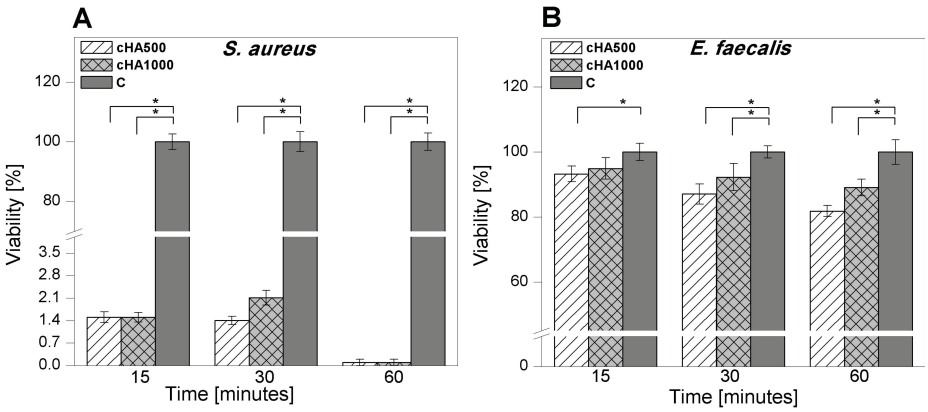

Figure 4. The impact of bone substitutes suspensions on the viability of *S.aureus* (A) and *E.faecalis* (B). Data are shown as a mean ± standard deviation (n = 3). *P < 0.05.

however, in case of *E. coli* both tested materials caused 100 % of growth inhibition after only 15 minutes of incubation. Generally, *E. coli* and *S. aureus* were significantly more sensitive to exposure to cHA/NPs powders than the *E. faecalis* strains. In the case of cHA500, *E. faecalis* viability was 93.2 % ± 2.4, 87.1 % ± 3.1 and 81.8 % ± 1.7 after 15, 30 and 60 minutes incubation time, respectively. Additionally, it was observed that the antibacterial activity against *S. aureus* and *E. faecalis* were slightly depended on the silver nanoparticles concentration. Both AgNPs doses elicited the similar antibacterial response. Moreover, it has been observed that the growths of both, *S. aureus* and *E. faecalis* were slightly affected by increasing the incubation time.

Disc diffusion test results (Figure 5) revealed that both samples exhibited high antimicrobial activity against *E. coli* and *S. aureus* strains, however, no inhibition zone was observed in the case of *E. faecalis*, which is consistent with previous antibacterial studies. Due to the presence of higher AgNPs concentration cHA1000 (*E. coli* 13.0 ± 0.22 mm and *S. aureus* 14.5 ± 0.17 mm) exhibited maximum activity as compared to cHA500 for both microorganism (*E. coli* 12.5 ± 0.20 mm and *S. aureus* 13.0 ± 0.17 mm), as opposed to *E. faecalis*, in case of which there was no zone of bacterial growth inhibition.

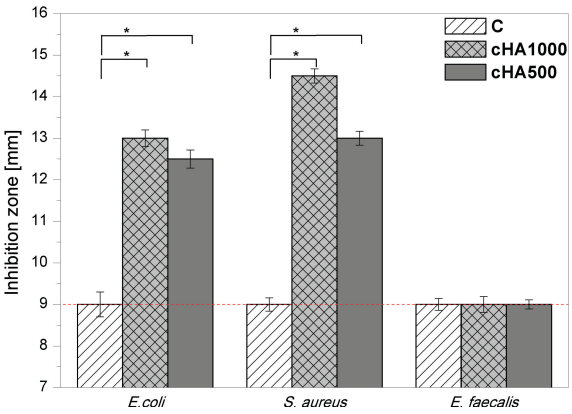

Figure 5. Disk diffusion test results of control (C), cHA500 and cHA1000 against *E. coli* and *S. aureus* and *E. faecalis*, respectively. Data are shown as a mean ± standard deviation (n = 3). *P < 0.05.

DISSCUSSION

X-ray diffraction phase composition analysis of the cHA and cHA/AgNPs powders demonstrated high crystallinity of the ceramics obtained in the three-step treatment of the material of animal origin. Applying the search-match program for all patterns, the only phase present in samples is found to be hydroxyapatite. The XRD analysis did not reveal TCP (tricalcium phosphate) formation. However, studies by Qian Jun He et al. confirm that the phase transition of carbonate hydroxyapatite may take place in a broad range of temperatures different to the temperatures specific for stoichiometric hydroxyapatite.[41] On the other hand, despite the better thermal stability and crystallinity, stoichiometric hydroxyapatite offers poorer bioactivity and osteoconductivity as compared to carbonate HA.[42]

IR analysis confirmed the presence of CO_3^{2-} groups in the analyzed materials. What is more, the experiments suggest conclusions that the phosphates are subject to isomorphous replacement of the phosphate group both at position A and B, which is indicated by ν_3 stretching mode of CO_3^{2-} (A-type or B-type), ν_2 bending mode of CO_3^{2-} (A-type) and ν_3 stretching mode of CO_3^{2-} (B-type). The absorption band at 869 cm^{-1} is typical of CO_3^{2-} anions, which partially take up positions of hydroxyl groups (A-type), while bands at 1489 cm^{-1} and 1413 cm^{-1} show partial replacement of phosphate groups (B-type). Based on the intensity ratio of individual absorption bands of the CO_3^{2-}, the IR analysis did not demonstrate new bonds resulting

from the modification of the surface of phosphates, which is indicative of the lack of introduction of ionic silver into the crystalline network of the phosphate. Moreover, the elemental analysis of the hydroxyapatite powders has demonstrated slight differences in Ca and P contents, which confirmed that the modification of the powders was superficial.

It is well known that silver nanoparticles exhibit an efficient antimicrobial activity which can be attributed to the high surface area providing a better contact with the microorganisms leading to enzymatic systems of the respiratory chain inhibition and alter DNA structure.[43] Another mechanism of antimicrobial reactivity of AgNPs is associated with the formation of free radicals and the release of silver ions which may lead to bacteria death.[44,45] Therefore, there are many scientific studies confirming the antibacterial activity of both ionic silver as well as their nanometric form.[46–48]

The study did not demonstrate a significant impact of the increased silver content in the suspension on the viability of *E. faecalis*. What is more, during incubation, only slight differences in the viability of *E. faecalis* were noted for cH500: 93.2 % ± 2.4, 87.1 % ± 3.1, and 81.8 % ± 1.7 after 15, 30, and 60 minutes of incubation, respectively. Obtained results revealed no effect of increased silver content on a mild growth inhibitory effect even in higher AgNPs concentration. The low sensitivity observed in *E. faecalis* could probably be explained by the biochemical and physiological characteristics of this bacteria, which is well known for its high level of resistance to a wide range of antimicrobial agents. However, *ex vivo* studies on bactericide effect of silver nanoparticles on *E. faecalis* performed by González-Luna et al. show that nanoparticles of 10 nm (537 μg/mL) + EDTA (17 %) applied as a final irrigation agent were effective for eliminating *E. faecalis* [48]. The possible conclusion is that in the case of *E. faecalis*, the bactericidal properties strongly depend on the size of nanoparticles. Enterococci are recognized to be resistant to many antibiotics. In consequence of expression of low-affinity penicillin-binding proteins enterococci present increased resistance to most cephalosporins and penicillins. Moreover, enterococci are intrinsically resistant to clindamycin, trimethoprim-sulfamethoxazole, and aminoglycosides. However, relatively rare resistance of *E. faecalis* to ampicillin and vancomycin does not preclude their clinical use. The best *in vitro* activity among of β-lactams utilizing in the treatment of *E. faecalis* infections is observed for aminopenicillins (ampicillin) and ureidopenicillins (piperacillin), followed by carbapenems (imipenem).[49] It is worth emphasizing that the proportion of infections that are antibiotics resistant depends on the bacteria strain.[50] Ampicilline activity against various strains of *E. faecalis* bacteria was examined by Jonathan et al.[51] The minimal inhibitory concentration (MIC) and minimal bactericidal concentration (MBC) determined by the authors were in the range of 0.5–8 μg/mL and 4–2048 μg/mL, respectively. The studies on trimethoprim bactericidal effect on ten randomly selected *E. faecalis* strains were carried out by Crider et al.[52] In accordance with this research, the MICs values varied from 0.063 to 4 μg/mL, while MBCs were in the range of 0.25 μg/mL–4 μg/mL. In the case of *E. coli* and *S. aureus*, our experiments revealed a high inhibition of the growth of these bacteria. In accordance with results obtained by Li et al.,[53] it can be assumed that AgNPs at the concentration of 10 μg/mL (5 nm) caused a total inhibition of respiratory chain dehydrogenases in *E. coli*. In light of the calculated yield of the surface modification of hydroxyapatite of 34.4 ug/mL for cHA500 and 54.6 ug/mL for cHA1000 resulting from the applied methods and of the size of nanoparticle agglomerates visible on SEM microphotographs, it may be concluded that due to high contents of Ag nanoparticles in the material, no viable bacterial cells were observed in the suspension. *E. coli* bacteria is a cause of a variety of nosocomial and community-acquired bacterial diseases including infections of the enteric and urinary tract, surgical site infections, and sepsis as well as systemic infections in humans. Nowadays, aminopenicillins, fluoroquinolones, third-generation cephalosporins, aminoglycosides and carbapenems are typically use in *E. coli* infections treatment.[54] However, in accordance with the current report regarding antimicrobial resistance in Europe, more than half of the reported *E. coli* isolates were resistant to at least one of the mentioned antimicrobial groups.[55] Antimicrobial effect of ampicilline on *E. coli (*ATCC 25922) was describe by Septama et al.[56] According to their research, MIC and MBC were 0.9 μg/mL 1.95 μg/mL, respectively. Comparison of levofloxacin and gepotidacin bactericidal activity towards *E. coli* and *S. aureus* was performed by Flamm et al.[57] Gepotidacin is a novel triazaacenaphthylene antibiotic revealing activity against drug-resistant pathogens. The MBCs of gepotidacin for all of the *S. aureus* isolates tested were all 0.25 μg/mL, while MICs were 0.5 μg/mL. The MBCs and MICs for the *E. coli* isolates examined were 2 μg/mL, and > 32 μg/mL, respectively. Levofloxacin bactericidal effect against *S. aureus* was strongly dependent on the strain type, while MBC and MIC values for *E. coli* were two times higher in comparison with gepotidacin. Performed by us antibacterial activity assessment of AgNPs against *S. aureus* colony showed that growth inhibition exceeded 98 %, which may be linked to the lack of outer membrane characteristic of Gram(+) bacteria, which makes it easier for Ag nanoparticles to act.[53] The result was consistent with the study of antibacterial effects of silver nanoparticles on *S. aureus* obtained by Li et al.[58] which indicate lost replicating ability of bacterial strain, causing death of bacteria cells.

CONCLUSION

The new approach for *in situ* preparation of hydroxyapatite surface modified with silver nanoparticles was developed to obtained antibacterial materials for wide application in the field of implantology and dentistry, especially in postoperative wound healing to prevent microbial infections. Taking into account the short time of production, the designed method can be considered as a new direction in effective antibacterial materials properties. No significant differences in crystal structure and chemical composition of cHA powders were indicated by XRD and FT-IR analysis, that confirmed no ionic substitution and chemical interaction between individual materials components. Additionally, SEM imaging demonstrated AgNPs presence on ceramic particles surface. Conducted research revealed antimicrobial properties of synthesized materials against *E. coli* and *S. aureus.*

Acknowledgment. The authors gratefully acknowledge financial support from National Science Centre in the frame of UMO-2016/21/D/ST8/01697.

REFERENCES

[1] L. A. Jacobsen, M. Kent, M. Lee, M. Mather, *Population Bulletin* **2011**, *66*, 1–2 https://doi.org/10.1007/s00289-010-0425-4

[2] G. K. Vincent, V. A. Velkoff, *Current Population Reports*, **2010**, Department of Commerce Economics and Statistics Administration U.S. Census Bureau

[3] M. Vallet-Regí, E. Ruiz-Hernández, *Adv. Mater.* **2011**, *23(44)*, 5177–5218. https://doi.org/10.1002/adma.201101586

[4] M. Saini, Y. Singh Y, P. Arora P, et al. *World J. Clin. Cases* **2015**, *3*, 1–9. https://doi.org/10.12998/wjcc.v3.i1.1

[5] C. F. Dunne, J. Gibbons J, P. Fitz, et al. *Ir. J. Med. Sci.* **2015**, *184(1)*, 125–133. https://doi.org/10.1007/s11845-014-1243-8

[6] C. Gao, S. Peng, P. Feng, et al. *Bone Res.* **2017**, *5,* 17059. https://doi.org/10.1038/boneres.2017.59

[7] N. Eliaz, N. Metoki, *Materials (Basel).* **2017**, *10*, 334–437. https://doi.org/10.3390/ma10040334

[8] M. Konop, T. Damps, A. Misicka, et al. *J. Nanomater.* **2016**, *2016*, 10 pages. https://doi.org/10.1155/2016/7614753

[9] M. Rai, A. Yadav, *Biotechnol. Adv.* **2009**, *27*, 76–83. https://doi.org/10.1016/j.biotechadv.2008.09.002

[10] M. Nakamura, R. Hiratai, T. Hentunen, et al. *ACS Biomater. Sci. Eng.* **2016**, *2*, 259–267. https://doi.org/10.1021/acsbiomaterials.5b00509

[11] M. Diaz, F. Barba, M. Miranda, et al. *J. Nanomater.* **2009**, *2009*, 6 pages.

[12] X. Zhang, G. H. Gubbels, R. A. Terpstra, et al. *J. Mater. Sci.* **1997**, *32*, 235–243. https://doi.org/10.1023/A:1018568308926

[13] R. Nirmala, F. A. Sheikh, M. A. Kanjwal, et al. *J. Nanopart. Res.* **2011**, *13*, 1917–1927. https://doi.org/10.1007/s11051-010-9944-z

[14] M. Sygnatowicz, K. Keyshar, A. Tiwari, *Biological and Biomedical Materials* **2010**, *62*, 65–70. https://doi.org/10.1007/s11837-010-0111-x

[15] N. Rameshbabu, T. S. S. Kumar, T. G. Prabhakar et al. *J. Biomed. Mater. Res. A*. **2007**, *80*, 581–591. https://doi.org/10.1002/jbm.a.30958

[16] A. Fakharzadeh, R. Ebrahimi-Kahrizsangi, B. Nasiri-Tabrizi et al. *Ceram. Int.* **2017,** *43,* 12588–12598. https://doi.org/10.1016/j.ceramint.2017.06.136

[17] K. Pluta, D. Malina, A. Sobczak-Kupiec, *Przemysł Chemiczny* **2016**, *95(6)*, 1147–1150. https://doi.org/10.15199%2F62.2016.6.12

[18] A. Sobczak-Kupiec, E. Olender, D. Malina et al. *Mater. Chem. Phys*. **2018**, *206*, 158–165. https://doi.org/10.1016/j.matchemphys.2017.12.020

[19] PN-R-64803:199P

[20] PN-80/C-87015

[21] A. Smith, F. J. Buchinsky, J.C. Post, *Otolaryngol. Head Neck Surg*. **2011**, *144*, 338–347. https://doi.org/10.1177/0194599810391620

[22] D. P. Lew, F. A. Waldvogel, *The Lancet* **2004**, *364*, 369–379. https://doi.org/10.1016/S0140-6736(04)16727-5

[23] R. Serra, R. Grande, L. Butrico et al. *Expert Rev. Anti. Infect. Ther.* **2015**, *13*, 605–613. https://doi.org/10.1586/14787210.2015.1023291

[24] G. E. Salvi, M.M. Fürst, N.P. Lang et al. *Clin. Oral Implants Res*. **2008**, *19*, 242–248. https://doi.org/10.1111/j.1600-0501.2007.01470.x

[25] P.H. Hsieh, M.S. Lee, K.Y. Hsu et al. *Clin. Infect. Dis*. **2009**, *49*, 1036–1043. https://doi.org/10.1086/605593

[26] I. N. Rôças, J. F. Jr. Siqueira, K. R. Santos. *J. Endod*. **2004**, *30*, 315–320. https://doi.org/10.1097/00004770-200405000-00004

[27] PN-EN 1040:2006E

[28] PN-EN 1276:2010E

[29] I. S. Neira, Y. V. Kolen'ko, O. I. Lebedev et al. *Cryst. Growth Des.* **2008**, *9*, 466–474. https://doi.org/10.1021/cg800738a

[30] S. Koutsopoulos, *J. Biomed. Mater. Res.* **2002**, *62*, 600–612. https://doi.org/10.1002/jbm.10280

[31] M. E. Fleet, L. Xiaoyang, *J. Solid State Chem.* **2004**, *177*, 3174–3182. https://doi.org/10.1016/j.jssc.2004.04.002

[32] I. Rehman, W. Bonfield, *J. Mater. Sci. Mater. Med.* **1997**, *8*, 1–4. https://doi.org/10.1023/A:1018570213546

[33] H. L. Jaber, A. S. Hammood, N. Parvin, *J. Aust. Ceram. Soc.* **2018**, *54*, 1–10. https://doi.org/10.1007/s41779-017-0120-0
[34] M. Mir, F. L. Leite, P. S. P. Herrmann et al. *Mat. Res.* **2012**, *15*, 622–627. https://doi.org/10.1590/S1516-14392012005000069
[35] E. Park, R. A. Condrate, D. Lee, *J. Mater. Sci. Mater. Med.* **2002**, *13*, 211–218. https://doi.org/10.1023/A:1013842415784
[36] R. L. Frost, A. Locke, W. N. Martens, *J. Raman Spectrosc.* **2008**, *39*, 901–908. https://doi.org/10.1002/jrs.1932
[37] U. Wehrmeister, D. E. Jacob, A. L. Soldati et al. *J. Raman Spectrosc.* **2010**, *42*, 926–935. https://doi.org/10.1002/jrs.2835
[38] B. O. Fowler, *Inorg. Chem.* **1974**, *13*, 207–214. https://doi.org/10.1021/ic50131a040
[39] G. M. Poralan Jr, J. E. Gambe, E. M. Alcantara et al. *IOP Conf. Ser.: Mater. Sci. Eng.* **2015**, 79, 012028. https://doi.org/10.1088/1757-899X/79/1/012028
[40] B. Viswanath, N. Ravishankar N, *Biomaterials.* **2008**, *29*, 4855–4863. https://doi.org/10.1016/j.biomaterials.2008.09.001
[41] Q. J. He, Z. L. Huang, X. K. Cheng et al. *Mater. Lett.* **2008**, *62(3)*, 539–542. https://doi.org/10.1016/j.matlet.2007.06.001
[42] I. Mayer, J. D. B. Featherstone, R. Nagler, *J. Solid State Chem.* **1985**, *56*, 230–235. https://doi.org/10.1016/0022-4596(85)90060-X
[43] R. Salomoni, P. Léo, A. F. Montemor et al. *Nanotechnol. Sci. Appl.* **2017**, *10*, 115–121. https://doi.org/10.2147/NSA.S133415
[44] C. Losasso, S. Belluco, V. Cibin et al. *Front Microbiol.* **2014**, *5*, 227. https://doi.org/10.3389/fmicb.2014.00227
[45] R. Krishnan, V. Arumugam, S. K. Vasaviah, *J. Nanomed. Nanotechnol*. **2015**, *6*, 1–4. https://doi.org/10.4172/2157-7439.1000285
[46] C. S. Ciobanu, S. L. Iconaru, P. Le Coustumer et al. *Nanoscale Res. Lett.* **2012**, *7*, 324. https://doi.org/10.1186/1556-276X-7-324
[47] T. A. Abalkhil, S. A. Alharbi, S. H. Salmen et al. *Biotechnol. Biotechnol. Equip.* **2017**, *31*, 411–417. https://doi.org/10.1080/13102818.2016.1267594
[48] P. González-Luna, H. A. Martínez-Castañón, N. V. Zavala-Alonso et al. *J. Nanomater.* **2016**, *7597295* https://doi.org/10.1155/2016/7597295
[49] C. J. Kristich, L. B. Rice, C. A. Arias in *Enterococci: From Commensals to Leading Causes of Drug Resistant Infection*, (Eds.: M. S. Gilmore MS, D. B. Clewell, Y. Ike et al.), Eye and Ear Infirmary, Massachusetts, **2014**, pp. 123-184.
[50] C. L. Ventola, P T. **2015**, *40*, 277–283.
[51] J. A. Sandoe, J. Wysome, A. P. West, *J. Antimicrob. Chemother*. **2006**, *57*, 767–770. https://doi.org/10.1093/jac/dkl013
[52] S. R. Crider, A. D. Colby, *Antimicrob. Agents Chemother.* **1985**, *27*, 71–75. https://doi.org/10.1128/AAC.27.1.71
[53] W. R. Li, X. B. Xie, Q. S. Shi et al. *Appl. Microbiol. Biotechnol.* **2010**, *85*, 1115–1122. https://doi.org/10.1007/s00253-009-2159-5
[54] J. D. Pitout, *Expert Rev. Anti Infect. Ther*. **2012**, *10*, 1165–1176. https://doi.org/10.1586/eri.12.110
[55] Annual report of the European Antimicrobial Resistance Surveillance Network (EARS-Net), Surveillance of antimicrobial resistance in Europe, **2017**.
[56] A. W. Septama, P. Panichayupakaranant, *J. Appl. Pharm. Sci.* **2017**, *7*, 64–68. https://doi.org/10.7324/JAPS.2017.71109
[57] R. K. Flamm, D. J. Farrell, P. R. Rhomberg, *Antimicrob. Agents Chemother.* **2017**, *61(7)*, e00468-17. https://doi.org/10.1128/AAC.00468-17
[58] W. R. Li, X. B. Xie, Q. S. Shi et al. *Biometals* **2011**, *24*, 135–141. https://doi.org/10.1007/s10534-010-9381-6